Proc. Arthropod. Embryol. Soc. Jpn. 53, 1–7 (2021)

ISSN 1341–1527

[REVIEW]

Bioluminescence Microscopy for the Visualization of Gene Expression Patterns and the Study of Embryonic Development*

Hirobumi SUZUKI

Olympus Corporation, Kuboyama 2–3, Hachioji, Tokyo 192–8512, Japan
E-mail: hirobumi2_suzuki@ot.olympus.co.jp

Abstract

Gene expression and its regulation are fundamental processes in cellular proliferation and differentiation, especially in morphogenesis and embryogenesis. Real-time gene expression analysis for live cells has been performed using a gene promoter assay with luciferase as the luminescent reporter. However the imaging of the promoter activity by microscopy is limited, since the intensity of the luminescence emitted from cells is too weak. To resolve this problem, a bioluminescence microscope was developed that was optimized for low-light imaging. The real-time imaging of gene expression during embryogenesis using bioluminescence microscopy contributes substantially to the elucidation of the phenomena and the interpretation of the mechanisms of developmental biology. For instance, it was elucidated that anisotropic tissue deformation along the proximal-distal axis occurred independently of cell proliferation in the chick limb development based on tissue morphology, cell proliferation, and sonic hedgehog signaling activity using bright field, fluorescence, and bioluminescence microscopies, respectively. However, the number of genes shown is limited by bioluminescence microscopy. Recently, a multi-omics method based on the workflow of systems biology has allowed for the integrated analysis of multiple-layer of organisms, from genes and expression to signaling pathways and metabolism. If image data of the phenotype layer can be incorporated into multi-omics analysis, bioluminescence microscopy could also be used for the integrated analysis of transcriptome and phenotype (morphogenesis or embryogenesis) layers.

Introduction

An organism composed of cells with various morphologies and functions is made from a single fertilized egg during embryogenesis. Therefore, gene expression and its regulation, including signal transduction, are fundamental processes in cellular proliferation and differentiation, especially in morphogenesis and embryogenesis (e.g. Davidson, 1976; Slack, 2001). In *Drosophila*, the mutation of homeotic genes results in morphological abnormalities were known. Studies on these genes have elucidated the relationships between the regulation of gene expression and morphogenesis related to the determination of the anterior-posterior axis, somitogenesis, and appendage limb formation. Furthermore, these genes have been demonstrated to be involved in morphogenesis and are conserved in mammals and other animals (e.g., Gehring, 1998).

Microscopic technologies have been used in these studies. While morphometry uses conventional bright-field observation, three-dimensional (3D) reconstruction is performed using a laser confocal fluorescence microscope. The structural and functional protein localization is imaged using immunostaining and fluorescence techniques. The study of cellular signal transduction and second messenger, such as Ca^{2+} or cyclic adenosine monophosphate (cAMP), dynamics is measured in live cells using real-time imaging with a fluorescent sensor probe. Molecular interactions and the translocation of signal transduction factors, such as the translocation of protein kinase C (PKC) from the cytoplasm to the plasma membrane for nuclear factor kappa-light polypeptide B (NF-κB) pathway activation, can be imaged using fluorescence microscopy with green fluorescent protein (GFP) (Goda et al., 2015). In gene expression analysis, however, the whole mount *in situ* hybridization method is performed using immunostaining and/or fluorescence microscopy. This method can be used to elucidate the detailed localization of cells expressing specific genes, and is applicable for fixed specimens. Therefore, the real-time imaging of gene expression activity in live specimens is required, as it is essential to describe the phenomena and its interpretation for morphogenesis or embryogenesis. Real-time gene expression analysis for live cells has been performed using a gene promoter assay with luciferase as the luminescent reporter. However the imaging of the promoter activity by

* Review of a special lecture presented at the 55th Annual Meeting of the Arthropodan Embryological Society of Japan, May 31– June 1, 2019 (Fuchu, Tokyo).

microscopy is limited, since the intensity of the luminescence emitted from cells is too weak. To resolve this problem, a bioluminescence microscope was developed that was optimized for low-light imaging. This system has been widely used for gene expression analysis in chronobiology (Yagita et al., 2010), neurobiology (Chang et al., 2016), developmental biology (Morishita et al., 2015), medical research (Sramek et al., 2011), signal transduction analysis (Sugiyama et al., 2014), molecular interaction (Compan et al., 2015), and radiation biology (Kiru et al., 2018).

This review briefly summarizes the history of low-light imaging of the promoter assay using luciferase and the specification of a bioluminescence microscope developed with bright luciferase development to improve luminescence imaging. The recent applications of bioluminescence microscopy in developmental biology are also discussed.

Bioluminescence microscopy for visualizing gene expression

In the late 1980s, the luciferase gene was first cloned from the American firefly, *Photinus pyralis* (de Wet et al., 1987). Luciferase is commonly used as a reporter enzyme for the promoter assays of gene expression (Brasier et al., 1989; de Wet et al., 1989; Alam and Cook, 1990). In the luciferase reporter assay, since the intensity of emitted light from cell population or cell lysate is measured as total luminescence with a photon-counting luminometer, it is impossible to simultaneously monitor the promoter activity of gene expression and cellular characteristics in the same cell as the image. Therefore, microscopic imaging is essential for the gene expression studies accompanied with cellular differentiation in embryonic development.

Advances in detector and digital imaging processing systems have made it possible for low-light imaging to be carried out using a high-sensitivity charge-coupled device (CCD) camera, such as liquid nitrogen cooled CCD cameras, photon-counting CCD cameras, or image-intensifying CCD cameras (Frawley et al., 1994; Thompson et al. (1995); Maire et al., 2000). This technology has allowed for the real-time image analysis of gene expression dynamics within a single cell and elucidated the heterogeneity of gene expression in cultured cells population for the prolactin gene promoter (Castaño et al., 1996; Takasuka et al., 1998), the L-pyruvate kinase gene promoter (Kennedy et al., 1997), and several other promoters (Rutter et al., 1995; White et al., 1995). In particular, the effectiveness of microscopic imaging has been demonstrated in clock genes analysis, namely in the oscillation of the clock and its phase shift at the single cell level. Circadian oscillations in the expression of clock genes are found not only in the central circadian pacemaker, suprachiasmatic nucleus (SCN), but also in peripheral tissues. Welsh et al. (2004) found that single fibroblasts are able to oscillate robustly, similar to SCN neurons, but lacked coupling in dissociated cell cultures, which led to a loss of synchrony among individual cells. The Notch signaling component gene, Hes 1, is cyclically expressed in the presomitic mesoderm and constitutes the somite segmentation clock. Masamizu et al. (2006) performed real-time bioluminescence microscopy of Hes 1 expression activity in the presomitic mesoderm and embryo of mice and found that cell-cell communication was essential for the synchronization and stabilization of cellular oscillators.

However, temporal and spatial resolution was not enough to observe of cellular biological events or detect single cells compared to conventional CCD cameras. Therefore, satisfactory analysis using bioluminescence microscopy is lacking at the single-cell level. Subsequently, an electron-multiplying CCD (EM-CCD) camera, which yields higher sensitivity and image quality, has been commercially released and used for bioluminescence microscopy (Kwon et al., 2010; Muranaka et al., 2013).

Development of a microscope optimized for bioluminescence imaging

Although the image sensors of low-light imaging cameras have been greatly improved over time, these improvements have not been made commercially available for microscopes. Because a microscope that has been designed with image quality prioritized over image brightness. In the mid-2000s, microscopes optimized for bioluminescence imaging were commercially released by Olympus (Tokyo, Japan) and Atto (Tokyo, Japan).

Generally, the degree of brightness (I) of an image is directly proportional to the square of the numerical aperture (NA) of the objective lens and inversely proportional to the square of the magnification (M) of the image. This can be represented as $I \propto (NA/M)^2$. Therefore, a higher NA and lower M yields brighter images. However, it is difficult to obtain both conditions. A higher NA objective lens has a shorter focal-length and, therefore, has a higher M. Thus, a high NA and a low M are mutual trade-offs. However, the value of NA/M is the same as the NA value of the imaging lens (tube lens), geometrically denoted as NA'. Therefore, a microscope with a high NA' (short focal-length imaging lens) allows for a higher NA and lower M without requiring further improvements to the objective lens. Thus, it was found that a higher value of I ($I > 0.01$) was required for the bioluminescence microscopy of single live cells (Suzuki et al., 2007; Ogoh et al., 2014; Suzuki et al., 2016a). This is the concept on which the design of the bioluminescence microscope was based. Fig. 1 shows the inverted bioluminescence microscope constructed in our studies (Luminoview LV200; Olympus). A stage-top incubator with temperature and CO_2 gas controllers is added to the sample stage. The observation area is covered with a dark box.

Figure 2 shows the bioluminescence images of U2OS cells expressing beetle luciferase CBG99, CBR, and Luc2 (Promega, Madison, WI, USA) at 37°C captured using LV200 and IX70 microscopes (Olympus) with a UPlanFLN 40× oil objective lens (Olympus) and DP70 color CCD camera (Olympus). The exposure times were 2 and 10 min for LV200 ($M = 8$, $I = 0.026$) and IX70 ($M = 40$, $I = 0.001$), respectively.

Thus, the bioluminescence images of cells expressing the luciferase gene could be captured using an LV200 microscope with a conventional color CCD camera. In this case, the M of the image was reduced by a power of 8 owing to the short focal-length imaging lens with a I value of 0.026. To equalize the I value between the LV200 and IX70 microscopes, a low M and high NA objective lens (e.g. 8 ×, NA 1.3) was required for IX70 (Ogoh et al., 2014; Suzuki et al., 2016a).

To show the spatial resolution of the bioluminescence images acquired using LV200, organelle targeted images were captured using an UPlanFLN 100 × oil objective lens (Olympus) and an ImagEM EM-CCD camera (C9100–13; Hamamatsu Photonics, Shizuoka, Japan). NanoLuc luciferase (Promega), which is 150-fold brighter than firefly luciferase (Hall et al., 2012), was used as a tag for organelle localization, similar to a fluorescent protein. Fig. 3 shows the bioluminescence images of NanoLuc fused with the nuclear localization sequence (NLS)

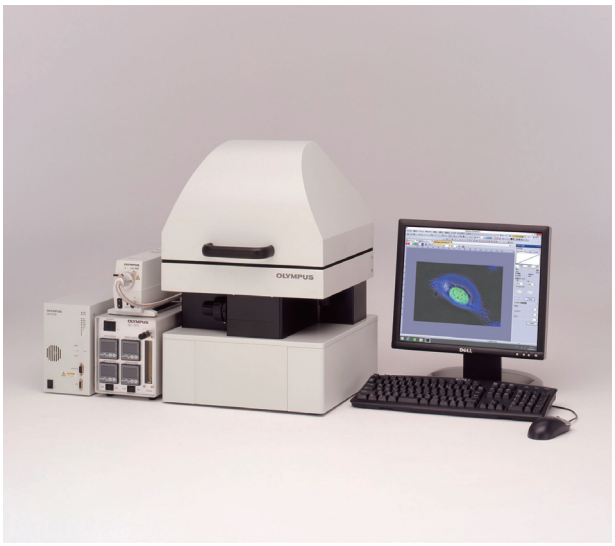

Fig. 1 Bioluminescence microscope, LV200 (Olympus). A stage-top incubator with temperature and CO_2 gas controllers is added to the sample stage. The observation area is covered with a dark box.

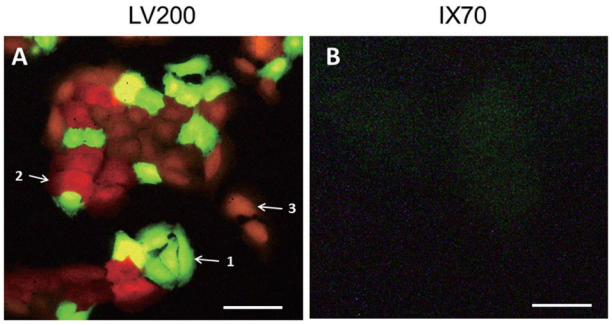

Fig. 2 Bioluminescence images of U2OS cells expressing beetle luciferase CBG99 (arrow 1), CBR (arrow 2), and Luc2 (arrow 3) at 37°C captured by LV200 and IX70 microscopes with a UPlanFLN 40 × oil objective lens and DP70 color CCD camera. The exposure times were 2 and 10 min for LV200 (M = 8, I = 0.026) and IX70 (M = 40, I = 0.001), respectively. D-Luciferin, 1 mM. Scales bar = 100 μm (A) and 20 μm (B). This figure was quoted and modified from Ogoh et al. (2014) and Suzuki et al. (2016a) with open access terms and conditions of Wiley and IntechOpen.

(Fig. 3A), the mitochondrial targeting sequence (subunit VIII of human cytochrome C oxidase, CoxVIII) (Fig. 3B), the endoplasmic reticulum resident protein, and the calreticulin with KDEL retrieval sequence (Fig. 3C) or no targeting sequence (Fig. 3D) with an exposure time from 300 msec to 1 sec in U2OS cells. Thus, the nucleus and cytoplasm were discriminated clearly, and mitochondria and the endoplasmic reticulum were observed in the cytoplasm (Ogoh et al., 2014; Suzuki et al., 2016a).

Development of bright and multi-color luciferase

In addition to the developments of low-light imaging cameras and microscopes, the development of bright luciferases also greatly contributed to bioluminescence microscopy, and color variants of luciferase further allowed to diversify bioluminescence microscopy in a manner similar to fluorescence microscopy. Since the initial cloning of the firefly luciferase gene, luciferase genes from many kinds of beetles (Coleoptera) have been cloned. The Jamaican click beetle, *Pyrophorus plagiophalam* has two sets of light organs. A pair of light organs on the dorsal surface of the prothorax and a single light organ in the ventral cleft of the abdomen emit yellowish green and orange luminescence, respectively. Four types of luciferase clones were isolated using the color of luminescence (green to orange) emitted by the light organs (Wood et al., 1989). Dual-color luciferase vectors (green and red color) were developed and released by Promega (Chroma-Luc vectors). Viviani et al. (1999a) also cloned luciferase genes

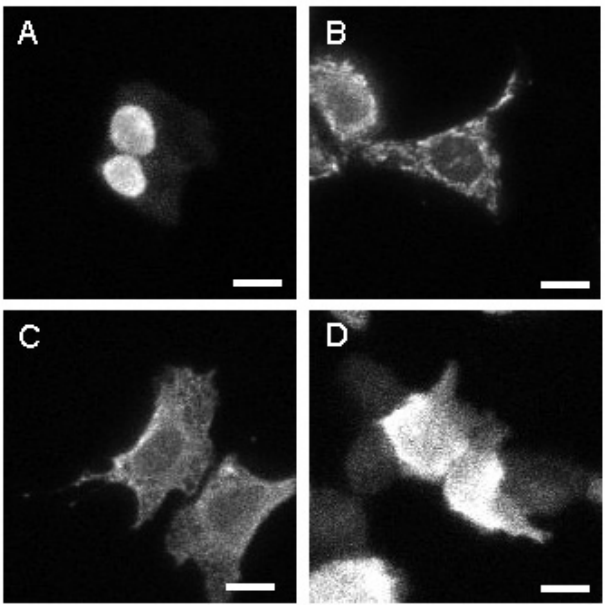

Fig. 3 Bioluminescence images of NanoLuc fused with NLS (A), CoxVIII (B), calreticulin (C), and no targeting sequence (D) in U2OS cells at 37°C. Images were captured using an LV200 microscope with an UPlanFLN 100× oil objective lens and an ImagEM EM-CCD camera. The binning of the EM-CCD camera was 1 × 1 (512 × 512 pixels), EM-gain was 1024, and exposure time was 300 msec (A, D), 500 msec (B), and 1 sec (C). Furimazine, 12.5 μM. Scale bar = 20 μm. This figure was quoted from Ogoh et al. (2014) and Suzuki et al. (2016a) with open access terms and conditions of Wiley and IntechOpen.

that emit green and red color luminescence from the Brazilian railroad warms, *Phrixothrix vivianii* and *P. hirtus*, respectively. Moreover, triple-color luciferase vectors (green, orange, and red color) were developed and released by Toyobo (Tripluc vectors; Osaka, Japan). Furthermore, a luciferase gene that displayed the most blue-shifted spectrum (λmax=538 nm) among the beetles was cloned from the Brazilian click beetle, *Pyrearinus termitilluminans* (Viviani et al., 1999b). It was optimized for bioluminescence imaging (Nakajima et al., 2010), which was 10-fold brighter than firefly luciferase and released by Toyobo (Emerald Luc vectors). Five luciferase genes were cloned from Japanese and Malaysian fireflies and modified for bioluminescence imaging, which emit a yellowish green to orange color luminescence and were 2- to 12-fold brighter than firefly luciferase, Luc2 (Promega). These were deposited at RIKEN BioResource Research Center (Tsukuba, Japan) under deposition numbers RDB14359–14363. Meanwhile, red-shifted firefly luciferase was developed and used to accomplish a video-rate *in vivo* bioluminescence imaging from neurons in the striatum of marmoset brain with D-luciferin substrate modification (Iwano et al., 2018).

In contrast to the beetle luciferase, which requires D-luciferin as a substrate, a luciferase originating from marine organisms requires coelenterazine and emits blue color luminescence. *Renilla* luciferase from a sea pansy was fused to yellow fluorescent protein (YFP) and used to construct a bioluminescence resonance energy transmittance (BRET) system (Hoshino et al., 2007). The fusion protein emitted yellow luminescence by BRET and was 4-fold brighter than the original *Renilla* luciferase by improving the quantum yield of light emission. Saito et al. (2012) constructed Nano-lantern, which is a chimera of enhanced *Renilla* luciferase and Venus (enhanced YFP) with a high BRET efficiency. It was 12-fold brighter than the *Renilla* luciferase, and its color derivatives allowed for the bioluminescent sensing of Ca^{2+}, cAMP and adenosine 5'-triphosphate (ATP) within live single cells in the same manner as in fluorescence microscopy (Takai et al., 2015; Suzuki et al., 2016b).

NanoLuc luciferase (Promega), obtained from the deep-sea shrimp, *Oplophorus gracilirostris* was 150-fold brighter than firefly luciferase with the modified coelenterazine, furimazine (Hall et al., 2012). Based on the NanoLuc, Robers et al. (2015) and Dixon et al. (2016) developed a protein-fragment complementation (PCA) system using circular permutated large and small fragments (NanoBRET, NanoBiT, HiBit; Promega). It allowed not only for low-level gene expression imaging but also for protein-protein interaction imaging in live cells.

Advantages and limitations of bioluminescence microscopy

Since bioluminescence microscopy requires no light excitation, it is substantively different from fluorescence microscopy. Firstly, bioluminescence microscopy has none of the autofluorescence problems associated with fluorescence microscopy which include a high background noise, a low signal/noise ratio, and low quantitativity. In fact, it was demonstrated that the autofluorescence of *Drosophila* embryo can cause problems during fluorescence microscopy (Akiyoshi et al., 2014). Secondly, bioluminescence microscopy is less phototoxic to live cells during their observation, since one of causes of the phototoxicity is due to generation of reactive oxygen species from fluorescent dyes by light irradiation (Icha et al., 2017). Therefore, bioluminescence microscopy permits non-lethal and long-term observation of live cells and is suitable for cell differentiation and embryonic studies. Thirdly, bioluminescence microscopy is suitable for the observation of light-sensitive cells, such as opsin-expressing cells (Sugiyama et al., 2014) or retina cells, as there is no need to consider the effect of fluorescent dye excitation light on photo-stimulation.

However, bioluminescence microscopy requires a substrate. Although the substrate is derived from the biological components of luminous organisms (firefly or sea pansy), a high concentration of substrate can affect cell viability. As such, it is necessary to consider the optimal concentration of substrate according to cell types and luciferase characteristics (Suzuki et al., 2017).

Although bioluminescence microscopy has been achieved by improving the imaging devices and luciferases, the emission intensity from cells remains lower than that obtained using fluorescence microscopy. Therefore, the spatio-temporal resolution of bioluminescence microscopy is limited compared to fluorescence microscopy.

Table 1 summarizes the characteristics of bioluminescence and fluorescence microscopies and highlights the use of bioluminescence microscopy as a powerful tool in cellular biology as well as its use as a complementary strategy to fluorescence microscopy.

Recent applications in developmental biology

Drosophila

Akiyoshi et al. (2014) constructed a transgenic *Drosophila*

Table 1 Substantive differences between bioluminescence and fluorescence microscopy.

	Bioluminescence	Fluorescence
Excitation energy	Chemical reaction	Photon
Auto-fluorescence	None	Affected
Photo-toxicity	None	Affected
Long term observation	Excellent	Acceptable
Observation of light-sensitive cells	Excellent	Acceptable
Brightness of image	Acceptable	Excellent
Spatio-temporal resolution	Acceptable	Excellent

carrying armadillo (arm) and luciferase fusion gene using a Gal4-UAS system. The *arm* is a segment polarity gene and encodes the mammalian homologue of β-catenin in mammals, which is a key mediator of the Wnt signaling pathway (Peifer et al., 1991) as well as being involved in cell–cell adhesion (Peifer et al., 1993). Although the *arm* expression has been characterized during the early stage of embryogenesis using mRNA *in situ* hybridization (Riggleman et al., 1989), Akiyoshi et al. (2014) demonstrated the continuous expression of *arm* throughout the entire process of embryogenesis using bioluminescence microscopy, and found that its expression was dramatically increased in the anterior midgut rudiment, the myoblasts of the dorsal/lateral musculature, and the posterior spiracle after stage 13 (Fig. 4), as well as in the cephalic region just before hatching at stage 17. Furthermore, they also found an *arm* expression pattern in embryos treated with ionomycin or 6-bromoindirubin-3-oxime (BIO), an inhibitor and an activator of Wnt/β-catenin signaling, respectively.

Chick

Sonic hedgehog (SHH) is expressed in the polarizing region of the vertebrate embryo and is essential for the anterior-posterior patterning of the limb bud (Tickle and Towers, 2017). Morishita et al. (2015) constructed a tissue deformation map of the chick limb development to characterize the geometrical tissue growth modes based on tissue morphology, cell proliferation, and SHH signaling activity using bright field, fluorescence, and bioluminescence microscopies, respectively. They found that SHH signaling activity changed dynamically through the developmental stage and growth mode shift, and demonstrated that anisotropic tissue deformation along the proximal-distal axis occurred independently of cell proliferation.

Zebrafish

The Wnt/β-catenin signaling gradient acts as a morphogen to determine the embryonic anterior-posterior axis in mammals (Huelsken et al., 2000). Akieda et al. (2019) identified unfit cells that appear spontaneously with abnormal Wnt/β-catenin activity and produce noise in the signaling gradient in zebrafish. These unfit cells were eliminated by apoptosis with Smad signaling and reactive oxygen species production via the communication of unfit cells with neighbouring fit cells using cadherin. Thus, the Wnt/β-catenin signaling gradient was established by elimination of the unfit cells. In this study, the real-time imaging of β-catenin gene expression in live embryos using bioluminescence microscopy contributed substantially to these findings.

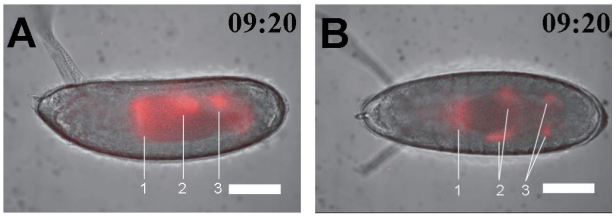

Fig. 4 Merged bright field and bioluminescence images of armadillo expression at stage 14 (9 h 20 min after fertilization) from lateral (A) and dorsal (B) side. Increased armadillo expression was observed in the anterior midgut rudiment (1), myoblasts of the dorsal/lateral musculature (2), and the posterior spiracle (3). Scale bar = 100 μm. This figure was quoted from Akiyoshi et al. (2014) with open access terms and conditions of Springer.

Perspectives

As shown in the previous "Recent applications in developmental biology" section, the real-time imaging of gene expression (promoter activity) during embryogenesis in a single specimen using bioluminescence microscopy contributes substantially to the elucidation of the phenomena and the interpretation of the mechanisms of developmental biology. Since the spatio-temporal resolution of real-time bioluminescence microscopy is limited, it is compensated by fluorescence microscopy using fixed tissue as the end point analysis. Therefore, the combination of bioluminescence and fluorescence microscopy in live cells or embryo is required. Goda et al. (2015, 2017) developed a method that combines bioluminescence and fluorescence microscopy by avoiding autofluorescence from D-luciferin, and showed the sequential imaging of the same cells from a signal transduction event (PKC translocation from cytosol to plasma membrane) using fluorescence microscopy to gene expression regulated by nuclear factor kappa-light polypeptide B (NF-κB) using bioluminescence microscopy, together with the cell morphology using bright field microscopy. However, problems with autofluorescence remained in the sample.

The transcriptome analysis using microarray or RNA sequencing methods has revealed that a large number of genes being expressed, and even the expression of all genes at once, as well as the activation of signal pathways can be specified based on the specific expressing gene groups, with a huge amount of data in biological systems analysis (Luo et al., 2009). Meanwhile, bioluminescence microscopy allows for the visualization of real-time genes expression patterns, together with the morphological changes of cells or tissues as images. However, the number of genes shown is limited. Recently, a multi-omics method based on the workflow of systems biology has allowed for the integrated analysis of multiple-layer of organisms, from genes and expression to signaling pathways and metabolism (Pinu et al., 2019). If image data of the phenotype layer can be incorporated into multi-omics analysis, bioluminescence microscopy could also be used for the integrated analysis of transcriptome and phenotype (morphogenesis or embryogenesis) layers.

Acknowledgements: I would like to thank Emeritus Professor Dr. Y. Kobayashi (Tokyo Metropolitan University) for providing me with the opportunity to present a special lecture in the 55th Annual Meeting of the Arthropodan Embryological Society of Japan at Fuchu in Tokyo in 2019. I would also like to thank my colleagues at Olympus Corporation for their technical assistance and fruitful discussions during

the development of the bioluminescence microscope.

References

Akieda, Y., S. Ogamino, H. Furuie, S. Ishitani, R. Akiyoshi, J. Nogami, T. Masuda, N. Shimizu, Y. Ohkawa and T. Ishitani (2019) Cell competition corrects noisy Wnt morphogen gradients to achieve robust patterning in the zebrafish embryo. Nature Communications, **10**, 4710, 1–17.

Akiyoshi, R., T. Kaneuch, T. Aigaki and H. Suzuki (2014) Bioluminescence imaging to track real-time armadillo promoter activity in live *Drosophila* embryos. Analytical and Bioanalytical Chemistry, **406**, 5703–5713.

Alam, J. and J.L. Cook (1990) Reporter genes: Application to the study of mammalian gene transcription. Analytical Biochemistry, **188**, 245–254.

Brasier, A.R., J.E. Tate and J.F. Habener (1989) Optimized use of the firefly luciferase assay as a reporter gene in mammalian cell lines. BioTechniques, **7**, 1116–1122.

Castaño, J.P., R.D. Kineman and L.S. Frawley (1996) Dynamic monitoring and quantification of gene expression in single, living cells: A molecular basis for secretory cell heterogeneity. Molecular Endocrinology, **10**, 599–605.

Chang, E., C. Pohling, A. Natarajan, T.H. Witney, J. Kaur, L. Xu, G. Gowrishankar, A.L. D'Souza, S. Murty, S. Schick, L. Chen, N. Wu, P. Khaw, P. Mischel, T. Abbasi, S. Usmani, P. Mallick and S.S. Gambhir (2016) AshwaMAX and Withaferin A inhibits gliomas in cellular and murine orthotopic models. Journal of Neuro-Oncology, **126**, 253–264.

Compan. V, S. Pierredon, B. Vanderperre, P. Krznar, I. Marchiq, N. Zamboni, J. Pouyssegur and J.C. Martinou (2015) Monitoring mitochondrial pyruvate carrier activity in real time using a BRET-based biosensor: investigation of the Warburg effect. Molecular Cell, **59**, 491–501.

Davidson, E. (1976) Gene Activity in Early Development. Academic Press, New York.

de Wet, J.R., K.V. Wood, M. DeLuca, D.R. Helinski and S. Subramani (1987) Firefly luciferase gene: structure and expression in mammalian cells. Molecular and Cellular Biology, **7**, 725–737.

Dixon, A.S., M.K. Schwinn, M.P. Hall, K. Zimmerman, P. Otto, T.H. Lubben, B.L. Butler, B.F. Binkowski, T. Machleidt, T.A. Kirkland, M.G. Wood, C.T. Eggers, L.P. Encell and K.V. Wood (2016) NanoLuc complementation reporter optimized for accurate measurement of protein interactions in cells. ACS Chemical Biology, **11**, 400–408.

Frawley, L.S., W.J. Faught, J. Nicholson and B. Moomaw (1994) Real time measurement of gene expression in living endocrine cells. Endocrinology, **135**, 468–471.

Gehring, W.J. (1998) Master Control Genes in Development and Evolution. Vail-Ballou Press, New York.

Goda, K., Y. Hatta-Ohashi, R. Akiyoshi, T. Sugiyama, I. Sakai, T. Takahashi and H. Suzuki (2015) Combining fluorescence and bioluminescence microscopy. Microscopy Research and Technique, **78**, 715–722.

Goda, K., T. Takahashi and H. Suzuki (2017) Combining fluorescence and bioluminescence microscopy to study the series of events from cellular signal transduction to gene expression. Current Protocols in Cell Biology, **77**, 4.35.1–4.35.16.

Hall, M.P., J. Unch, B.F. Binkowski, M.P. Valley, B.L. Butler, M.G. Wood, P. Otto, K. Zimmerman, G. Vidugiris, T. Machleidt, M.B. Robers, H.A. Benink, C.T. Eggers, M.R. Slater, P.L. Meisenheimer, D.H. Klaubert, F. Fan, L.P. Encell and K.V. Wood (2012) Engineered luciferase reporter from a deep sea shrimp utilizing a novel imidazopyrazinone substrate. ACS Chemical Biology, **7**, 1848–1857.

Hoshino, H., Y. Nakajima and Y. Ohmiya (2007) Luciferase-YFP fusion tag with enhanced emission for single-cell luminescence imaging. Nature Methods, **4**, 637–639.

Huelsken, J., R. Voge, V. Brinkmann, B. Erdmann, C. Birchmeier and W. Birchmeier (2000) Requirement for β-catenin in anterior-posterior axis formation in mice. Journal of Cell Biology, **148**, 567–578.

Icha, J., M. Weber, J.C. Waters and C. Norden (2017) Phototoxicity in live fluorescence microscopy, and how to avoid it. BioEssays, **39**, 1700003, 1–15.

Iwano, S., M. Sugiyama, H. Hama, A. Watakabe, N. Hasegawa, T. Kuchimaru, K.Z. Tanaka, M. Takahashi, Y. Ishida, J. Hata, S. Shimozono, K. Namiki, T. Fukano, M. Kiyama, H. Okano, S. Kizaka-Kondoh, T.J. McHugh, T. Yamamori, H. Hioki, S. Maki and A. Miyawaki (2018) Single-cell bioluminescence imaging of deep tissue in freely moving animals. Science, **359**, 935–939.

Kennedy, H.J., B. Viollet, I. Rafiq, A. Kahn and G.A. Rutter (1997) Upstream stimulatory factor-2 (USF2) activity is required for glucose stimulation of L-pyruvate kinase promoter activity in single living islet β-cells. Journal of Biological Chemistry, **272**, 20636–20640.

Kiru, L., T.J. Kim, B. Shen, F.T. Chin and G. Pratx (2018) Single-cell imaging using radioluminescence microscopy reveals unexpected binding target for [18F]HFB. Molecular Imaging and Biology, **20**, 378–387.

Kwon, H. J., T. Enomoto, M. Shimogawara, K. Yasuda, Y. Nakajima and Y. Ohmiya (2010) Bioluminescence imaging of dual gene expression at the single-cell level. BioTechniques, **48**, 460–462.

Luo, W., M.S. Friedman, K. Shedden, K.D. Hankenson and P.J. Woolf (2009) GAGE: generally applicable gene-set enrichment for pathway analysis. BMC Bioinformatics, **10**, 161, 1–17.

Maire, E., E. Lelièvre, D. Brau, A. Lyons, M. Woodward, V. Fafeur and B. Vandenbunder (2000) Development of an ultralow-light-level luminescence image analysis system for dynamic measurements of transcriptional activity in living and migrating cells. Analytical Biochemistry, **280**, 118–127.

Masamizu, Y., T. Ohtsuka, Y. Takashima, H. Nagahara, Y. Takenaka, K. Yoshikawa, H. Okamura and R. Kageyama (2006) Real-time imaging of the somite segmentation clock: Revelation of unstable oscillators in the individual presomitic mesoderm cells. Proceedings of the National Academy of Sciences of the United States of America, **103**, 1313–1318.

Morishita, Y., A. Kuroiwa and T. Suzuki (2015) Quantitative analysis of tissue deformation dynamics reveals three characteristic growth modes and globally aligned anisotropic tissue deformation during chick limb development. Development, **142**, 1672–1683.

Muranaka, T., S. Kubota and T. Oyama (2013) A single-cell bioluminescence imaging system for monitoring cellular gene

expression in a plant body. Plant Cell Physiology, **54**, 2085–2093.

Nakajima, Y., T. Yamazaki, S. Nishii, T. Noguchi, H. Hoshino, K. Niwa, V.R. Viviani and Y. Ohmiya (2010) Enhanced beetle luciferase for high-resolution bioluminescence imaging. PLoS ONE, **5**, e10011, 1–11.

Ogoh, K., R. Akiyoshi, May-Maw-Thet, T. Sugiyama, S. Dosaka, Y. Hatta-Ohashi and H. Suzuki (2014) Bioluminescence microscopy using a short focal-length imaging lens. Journal of Microscopy, **253**, 191–197.

Peifer, M., C. Rauskolb, M. Williams, B. Riggleman and E. Wieschaus (1991) The segment polarity gene armadillo interacts with the wingless signalling pathway in both embryonic and adult pattern formation. Development, **111**, 1029–1043.

Peifer, M., S. Orsulic, D. Sweeton and E. Wieschaus (1993) A role for the *Drosophila* segment polarity gene armadillo in cell adhesion and cytoskeletal integrity during oogenesis. Development, **118**, 1191–1207.

Pinu, F.R., D.J. Beale, A.M. Paten, K. Kouremenos, S. Swarup, H.J. Schirra and D. Wishart (2019) Systems biology and multi-omics integration: Viewpoints from the metabolomics research community. Metabolites, **9**, E76, 1–31.

Riggleman, B., E. Wieschaus and P. Schedl (1989) Molecular analysis of the armadillo locus: Uniformly distributed transcripts and a protein with novel internal repeats are associated with a *Drosophila* segment polarity gene. Genes and Development, **3**, 96–113.

Robers, M.B., M.L. Dart, C.C. Woodroofe, C.A. Zimprich, T.A. Kirkland, T. Machleidt, K.R. Kupcho, S. Levin, J.R. Hartnett, K. Zimmerman, A.L. Niles, R.F. Ohana, D.L. Daniels, M. Slater, M.G. Wood, M. Cong, Y.Q. Cheng and K.V. Wood (2015) Target engagement and drug residence time can be observed in living cells with BRET. Nature Communications, **6**, 10091, 1–10.

Rutter, G.A., M.R.H. White and J.M. Tavaré (1995) Involvement of MAP kinase in insulin signaling revealed by non-invasive imaging of luciferase gene expression in single living cells. Current Biology, **5**, 890–899.

Saito, K., Y.F. Chang, K. Horikawa, N. Hatsugai, Y. Higuchi, M. Hashida, Y. Yoshida, T. Matsuda, Y. Arai and T. Nagai (2012) Luminescent proteins for high-speed single-cell and whole-body imaging. Nature Communications, **3**, 1262, 1–9.

Slack, J.M.W. (2001) Essential Developmental Biology. Blackwell Science, Oxford.

Sramek, C, M. Mackanos, R. Spitler, L.S. Leung, H. Nomoto, C.H. Contag and D. Palanker (2011) Non-damaging retinal phototherapy: Dynamic range of heat shock protein expression. Investigative Opthalmology and Visual Science, **52**, 1780–1787.

Sugiyama, T. T. Takahashi and H. Suzuki (2014) Light-induced rapid Ca^{2+} response and MAPK phosphorylation in the cells heterologously expressing human OPN5. Scientific Reports, **4**, 5352, 1–10.

Suzuki, H., S. Dosaka, Y. Ohashi-Hatta and T. Sugiyama (2007) Luminescence microscope for reporter assay for single live cells. In A.A. Szalay, P.J. Hill, L.J. Kricka, and P.E. Stanley (eds.), Bioluminescence and Chemiluminescence: Chemistry, Biology and Applications, pp. 53–56. World Scientific Publishing, Singapore.

Suzuki, H., May-Maw-Thet, Y. Hatta-Ohashi, R. Akiyoshi and T. Hayashi (2016a) Bioluminescence microscopy: Design and Applications. In J. Thirumalai (ed.), Luminescence - An Outlook on the Phenomena and their Applications, pp. 333–349. IntechOpen, Croatia.

Suzuki, K., T. Kimura, H. Shinoda, G. Bai, M.J. Daniels, Y. Arail, M. Nakano and T. Nagai (2016b) Five color variants of bright luminescent protein for real-time multicolor bioimaging. Nature Communications, **7**, 13718, 1–10.

Suzuki, H., R. Akiyoshi and K. Ogoh (2017) Bioluminescence microscopy in live cells: consideration of experimental factors and practical recommendations. In L.V. Berhardt (ed.), Advances in Medicine and Biology, Vol. 108, pp. 101–115. Nova Science Publishers, New York.

Takai, A., M. Nakano, K. Saito, R. Haruno, T.M. Watanabe, T. Ohyanagie, T. Jine, Y. Okada and T. Nagai (2015) Expanded palette of Nano-lanterns for real-time multicolor luminescence imaging. Proceedings of the National Academy of Sciences of the United States of America, **112**, 4352–4356.

Takasuka, N., M.R.H. White, C.D. Wood, W.R.Robertson and J.R.E. Davis (1998) Dynamic changes in prolactin promoter activation in individual living lactotrophic cells. Endocrinology, **139**, 1361–1368.

Thompson, E.M., P. Adenot, F.I. Tsuji and J.P. Renard (1995) Real time imaging of transcriptional activity in live mouse preimplantation embryos using a secreted luciferase. Proceedings of the National Academy of Sciences of the United States of America, **92**, 1317–1321.

Tickle, C. and M. Towers (2017) Sonic hedgehog signaling in limb development. Frontiers in Cell and Developmental Biology, **5**, 14, 1–19.

Viviani, V.R., E.J.H. Bechara and Y. Ohmiya (1999a) Cloning, sequence analysis, and expression of active *Phrixothrix* railroad-worms luciferases: Relationship between bioluminescence spectra and primary structures. Biochemistry, **38**, 8271–8279.

Viviani, V.R., A.C. Silva, G.L. Perez, R.V. Santelli, E.J. Bechara and F.C. Reinach (1999b) Cloning and molecular characterization of the cDNA for the Brazilian larval click-beetle *Pyrearinus termitilluminans* luciferase. Photochemistry and Photobiology, **70**, 254–260.

Welsh, D.K., S.H. Yoo, A.C. Liu, J.S. Takahashi and S.A. Kay (2004) Bioluminescence imaging of individual fibroblasts reveals persistent, independently phased circadian rhythms of clock gene expression. Current Biology, **14**, 2289–2295.

White, M.R.H., M. Masuko, L. Amet, G. Elliott, M. Braddock, A.J. Kingsman and S.M. Kingsman (1995) Real-time analysis of the transcriptional regulation of HIV and hCMV promoters in single mammalian cells. Journal of Cell Science, **108**, 441–455.

Wood, K.V., Y.A. Lam, H.H. Seliger and W.D. McElroy (1989) Complementary DNA coding click beetle luciferase can elicit bioluminescence of different colors. Science, **244**, 700–702.

Yagita, K., K. Horie, S. Koinuma, W. Nakamura, I. Yamanaka, A. Urasaki, Y. Shigeyoshi, K. Kawakami, S. Shimada, J. Takeda and Y. Uchiyama (2010) Development of the circadian oscillator during differentiation of mouse embryonic stem cells in vitro. Proceedings of the National Academy of Sciences of the United States of America, **107**, 3846–3851.